Begell House, Inc. Publishers

Journal Production
50 Cross Highway
Redding, CT 06896
Phone: 1-203-938-1300
Fax: 1-203-938-1304
Begell House Production Contact : journals@begellhouse.com

Dear Corresponding Author,

Attached is the corresponding author pdf file of your article that has been published.

Please note that the pdf file provided is for your own personal use and is not to be posted on any websites or distributed in any manner (electronic or print). Please follow all guidelines provided in the copyright agreement that was signed and included with your original manuscript files.

Any questions or concerns pertaining to this matter should be addressed to journals@begellhouse.com

Thank you for your contribution to our journal and we look forward to working with you again in the future.

Sincerely,
Michelle Amoroso
Michelle Amoroso
Production Department

Journal of Porous Media, 16 (7): 607–617 (2013)

GAS DIFFUSIVITY IN POROUS MEDIA: DETERMINATION BY MERCURY INTRUSION POROSIMETRY AND CORRELATION TO POROSITY AND PERMEABILITY

Zhiye Gao,[1] Qinhong Hu,[1,] & Hecheng Liang[2]*

[1]*Department of Earth and Environmental Sciences, University of Texas at Arlington, Arlington, Texas 76019, USA*

[2]*School of Environmental Studies, China University of Geosciences, Wuhan, 430074, China*

[*]Address all correspondence to Qinhong Hu E-mail: maxhu@uta.edu

Original Manuscript Submitted: 10/8/2012; Final Draft Received: 2/7/2013

Much effort has been extended on diffusivity measurement because diffusion can dominate mass transport in porous media of low hydraulic conductivity. The main purpose of this work is to derive the gas diffusivities of building materials, rocks and sediments using the average pore size measured by mercury intrusion porosimetry (MIP). MIP has been utilized for decades to obtain the poresize distribution of porous media. We performed triplicate MIP tests on concrete and Berea sandstone to evaluate the repeatability of MIP data. Gas diffusivity results are consistent with literature data using the gas diffusion methods. Our results show that the relationship between gas diffusivity and porosity is analogous to Archie's law and that two groups of rocks are differentiated according to the cementation factor m value in an Archie's-type relationship. It also appears that gas diffusivity exhibits an increasing trend with an increase of permeability, and two different exponential relationships exist between permeability and porosity for these two groups of rocks.

KEY WORDS: *MIP, gas diffusivity, effective diffusion coefficient, permeability, porosity*

1. INTRODUCTION

Diffusion and advection are two important processes controlling mass transport in porous media. The relative contribution of these two processes depends primarily on the properties of the porous medium. For example, Gillham et al. (1984) pointed out that diffusion dominates mass transport when seepage velocity is on the order of 0.005 m/year, which is higher than that of many rocks. Generally, diffusion may be the dominant transport process in porous media with very low permeability (Boving and Grathwohl, 2001). As a result, a comprehensive understanding of diffusion processes in porous media becomes essential for waste disposal, carbon dioxide storage, evaluation of building materials, and gas production from unconventional reservoirs (e.g., Shackelford, 1991; Seo et al., 2005; Busch et al., 2008; Cui et al., 2009).

The measurement of diffusivity could be achieved by using liquid-phase or gas-phase tracers. Shackelford (1991) reviewed the methods used to measure effective diffusion coefficients of chemical species and summarized the advantages and disadvantages of each method. The diffusion chamber method has been used to make gas diffusivity measurements in unconsolidated (Rolston and Moldrup, 2002) and consolidated media (Peng et al., 2012).

Mu et al. (2008) indicated that the effective diffusion coefficient is strongly dependent on pore size when the average pore size is less than 1 μm, which is the situation for many rocks. As an advanced tool in characteriz-

1091–028X/13/$35.00

ing poresize distribution, mercury intrusion porosimetry (MIP) could provide useful information on pore structure (such as porosity and average pore size). Compared with traditional methods (e.g., the gas diffusion approach), determination of gas diffusivity from the pore-size information obtained through MIP is less time consuming (usually requiring less than 2 hours), and MIP covers a wide range of pore sizes (from 10^{-4} to 10^{-9} m), making it more convenient and applicable. Using MIP, Seo et al. (2005) evaluated the effective diffusion coefficient in building materials and absorbents, and presented the effective diffusion coefficients of different gases for these materials. In this work we investigate the effective gas diffusion coefficients in different types of rocks (sedimentary and igneous) and unconsolidated sediments with different grain sizes, and in building materials. In addition, we explore the correlation of gas diffusivity to porosity and permeability.

2. MATERIALS

Three types of porous media (listed in Table 1) were used in our research. They included two building materials, eight rocks, and four unconsolidated sediments with different grain sizes. All the consolidated samples were reduced to small pieces (>5 mm but <15 mm) according to the dimension of the cylindrical bowl of a penetrometer, which is the sample container by MIP. Sediments were collected from the vadose zone (∼3–4 m below ground surface) of the Integrated Field-Scale Research Challenge site at the Hanford 300 Area in Richland WA, and were sieved into four groups of <75 μm, 75–500 μm, 500 μm–2 mm and <2 mm (Du et al., 2012). During MIP tests, these unconsolidated samples were placed in a penetrometer specially designed for powder samples.

Before MIP testing, all the samples were oven-dried at 60°C for at least 48 hours, and were then cooled to room temperature (∼22.5°) in a desiccator. Porosity, average pore size d_a (defined in Section 3.2.2) and median pore size (d_{50}), which is the pore diameter corresponding to 50% mercury saturation, were obtained from the results directly reported by MIP. The calculation of permeability and diffusivity was based on these poresize data, as described in detail in the next section

3. GAS DIFFUSIVITY: THEORETICAL BACKGROUND AND MEASUREMENT BY MIP

3.1 Definition of Diffusivity

Gas diffusion in porous media is a process caused by the random thermal motion of gas molecules, which can be described by Fick's first law, which takes the form of Eq. (1) if the diffusion occurs under steadystate conditions in a one-dimensional system at uniform temperature and pressure (Boving and Grathwohl, 2001):

$$Fg = -D_e \frac{\partial C}{\partial x}, \tag{1}$$

where F_g is the diffusive gas flux [M·L^{-2}·T^{-1}]; D_e is the effective gas diffusion coefficient in the porous medium [L^2·T^{-1}]; C denotes gas concentration in the pore [M·L^{-3}]; and x denotes distance [L].

TABLE 1: Samples used in this study

Sample		Source
Building materials	Concrete	Home Depot
	Red brick	Triangle Brick Company, Durham, NC
Rocks	Limestone	Hanover Park, MD
	Dolomite	Unknown
	Indiana sandstone	Gas storage formation, Lombard, IL
	Berea sandstone	Berea Quarry, OH
	Gray chalk	Negev Desert, Israel
	White chalk	Negev Desert, Israel
	Tuff	Yucca Mountain, NV
	Mudstone	Hokkaido, Japan
Unconsolidated sediments	<2 mm	Hanford Site, Richland, WA
	500 μm–2 mm	Hanford Site, Richland, WA
	75–500 μm	Hanford Site, Richland, WA
	<75 μm	Hanford Site, Richland, WA

Defined as the ratio of D_e to the gas diffusion coefficient in air, D_a, gas diffusivity (D') is often expressed as an exponential function of porosity (Grathwohl 1998), in a form analogous to Archie's law;

$$\frac{D_e}{D_a} = D' = \varphi_a^m, \tag{2}$$

where φ_a is air-filled porosity and m is an empirical exponent called cementation factor

The m value in Archie's relationship [Eq. (2)] depends on the pore geometry of the porous media and several different m values are reported in the literature (Peng et al., 2012). For example, Archie (1942) reported m value from 1.8 to 2.0 for consolidated sand, and Adler et al. (1992) obtained an m value as 1.64 for Fontainebleau sandstone.

3.2 Theoretical Background

3.2.1 MIP as a Characterization Tool

As a well-developed characterization tool, MIP has received attention from many researchers and is commonly applied in pharmacy, civil engineering and reservoir engineering (Westermarck et al., 1998; Tsakiroglou and Payatakes, 2000; Kumar and Bhattacharjee, 2004).

Because of its nonwetting property to most geological materials, mercury will not invade pores unless it is applied with an external pressure. The diameter of the pores invaded by mercury is inversely proportional to the applied pressure, which is expressed as the following equation developed by Washburn (1921), based on the assumption that all pores in porous media are cylindrical in shape:

$$\Delta P = -\frac{2\gamma\cos\theta}{R}, \tag{3}$$

where ΔP is the pressure difference across the curved mercury interface (dyne/cm^2); γ is the surface tension of mercury (485 dynes/cm); θ is the contact angle (130°) between mercury and the porous media, as reported by Ellison et al. (1967); and R is the corresponding pore radius (cm).

Micromeritics AutoPore IV 9510, the instrument used to perform MIP tests in this work, can generate pressure as high as 413 MPa (60-000 psia) during high-pressure analysis. According to Eq. (3), the pore diameter corresponding to this pressure is about 3 nm. The largest pore diameter measurable by MIP during low-pressure analysis is about 300 microns.

However, MIP testing has its shortcomings. Shi and Winslow (1985) pointed out that changes of contact angle and damage to cement paste during the intrusion process should be considered, and that this may complicate MIP data processing. The ideal cylindrical pore shape may not be true (Rojas et al., 2012), and an ink-bottle effect in MIP has been reported by many researchers (e.g., Moro and Böhni, 2002). The ink-bottle effect will result in an underestimation of large pores (e.g., Zhou et al., 2010).

3.2.2 Determination of Gas Diffusivity from MIP Data

Gas diffusion within pore spaces usually has two forms: Knudsen diffusion and normal diffusion (Evans et al., 1961). The type of diffusion likely to be dominant depends on the relative length of the pore diameter and the mean free path of the gas molecule (Moore and Alzayadi, 1975). If the mean free path of the gas molecule is much larger than the pore diameter it passes through, then the collision of the gas molecules with the pore walls (i.e., Knudsen diffusion) will be the dominant process. In contrast, if the mean free path is much smaller than the pore diameter, the collisions between gas molecules (normal diffusion) will control the diffusion process, while the Knudsen diffusion is negligible. However, in many real situations these two diffusion mechanisms can simultaneously contribute to the gas diffusion in pore spaces.

For convenience, we arbitrarily chose O_2 with D_a = 2.04×10^{-5} m^2/s as the pseudogas in the derivation process of this work. The mean free path of oxygen at standard ambient temperature and pressure (25°, 1 bar) is about 0.073 μm and our MIP results show that the average pore sizes of most samples are at or below this length scale (Table 3). Because of this, Knudsen diffusion is considered in order to accurately predict diffusivity; this is shown in Eq. (4) which is known as the Bosanquet relation (Pollard and Present, 1948):

$$\frac{1}{D} = \frac{1}{D_a} + \frac{1}{D_{KA}}, \tag{4}$$

where D is the gas diffusion coefficient [$L^2 \cdot T^{-1}$] D_a denotes the gas diffusion coefficient in air [$L^2 \cdot T^{-1}$] and D_{KA} is the Knudsen diffusion coefficient [$L^2 \cdot T^{-1}$].

The Knudsen diffusion coefficient, D_{KA}, depends on the temperature, molecular weight of gas (O_2) and average pore size of the porous medium, as expressed by Eq. (5) (Cunningham and Williams 1980; Kast and Hohenthanner 2000; Seo et al., 2005)

$$D_{KA} = 48.5 d_a \sqrt{\frac{T}{M}}, \tag{5}$$

where T is absolute temperature (K); M is molecular weight of gas (g/mol); and d_a is the average pore diameter (m) that is calculated according to the following equation in MIP:

$$d_a = \frac{4V}{A} \times 10^{-6}, \tag{6}$$

where V is the total intrusion volume (mL/g); and A is the total pore area (m^2/g).

The effective diffusion coefficient was calculated according to the following equation (Evans et al., 1961; Carniglia, 1986; Seo et al., 2005):

$$D_e = \frac{\varphi_a}{\tau} D, \tag{7}$$

where τ is the tortuosity factor given by Carniglia (1986) as follows:

$$\tau = 2.23 - 1.13\varphi_a \quad (\text{applicable for } 0.05 \leq \varphi_a \leq 0.95). \tag{8}$$

We should point out that the derivation of Eq. (8) is based on the assumption that cylindrical diffusion paths prevail in the given porous media (Carniglia 1986).

In summary, after obtaining the average pore size and porosity from MIP tests, we were able to calculate gas diffusivity according to Eqs. (2) and (4)–(8).

3.2.3 Permeability Calculation from MIP Data

Absolute (or intrinsic) permeability, a measure of the relative ease with which a porous medium can transmit a fluid under a potential gradient, is only a property of the porous medium and depends on the pore structure. Many researchers have attempted to derive permeability from MIP data (Kolodzie, 1980; Swanson, 1981; Katz and Thompson, 1986, 1987). Among them, Katz and Thompson (1986, 1987) introduced the following equation (referred to as KT method hereafter) to calculate the absolute permeability based on MIP data:

$$k = \frac{1}{89} (L_{\max})^2 \left(\frac{L_{\max}}{L_c} \right) \varphi S (L_{\max}), \tag{9}$$

where k is absolute permeability (Darcy); $L_{\max}$ is the pore diameter (μm) at which hydraulic conductance is maximum; L_c is the characteristic length (μm) which is the pore diameter corresponding to the threshold pressure P_t; φ is porosity and S ($L_{\max}$) represents the fraction of connected pore space composed of pore width of size $L_{\max}$ and larger.

Webb (2001) described the KT method [Eq. (9)] in detail for predicting permeability; we obtained the permeability of each sample according to the KT method. The relationship between permeability and porosity will be presented in the Results and Discussion section.

4. RESULTS AND DISCUSSION

4.1 Repeatability of MIP Tests

Berea sandstone and concrete samples were selected for triplicate MIP testing and the remaining samples were tested only once. Ideally, a repeatability test should be carried out on the same sample as previously tested. This is not possible in the case of MIP testing, as the samples remain contaminated with mercury after any MIP test, and thus cannot be used in a subsequent MIP test. Therefore, we chose three representative samples from the same rock type or building material to evaluate the repeatability of MIP. The experimental result of triplicate MIP tests performed on Berea sandstone and concrete are shown in Fig. 1, and the pore-size results of the repeatability tests are summarized in Table 2.

In Fig. 1, the cumulative intrusion curves of Berea sandstone 2 and 3 (B2 and B3) are overlapped with each other while Berea sandstone 1 (B1) shows different behavior. This is in accordance with Table 2, in which the average pore diameter of B1 is smaller than B2 and B3. This difference probably reflects the heterogeneity of the Berea sandstone. The results of the three samples of concrete are acceptable considering the small pore sizes and heterogeneity of concrete.

4.2 Gas Diffusivity

Table 3 presents our results of several important parameters, such as diffusivity (D') and the cementation factor (m values), for the total of 14 samples. Among consolidated samples, Berea sandstone has the highest diffusivity (D' = 0.104) while tuff has the lowest (D' = 0.007). Peng et al. (2012) measured the effective diffusion coefficients of the same samples using the diffusion chamber method with oxygen. The comparison of results from the two approaches is shown in Fig. 2. Except for one sample of unconsolidated sediment (size fraction 500 μm–2 mm) which shows a marked deviation, and limestone which was not available in Peng et al. (2012), most of our results are distributed equally near the straight line with slope = 1. This supports the validity of the derivation method of determining effective diffusion coefficient

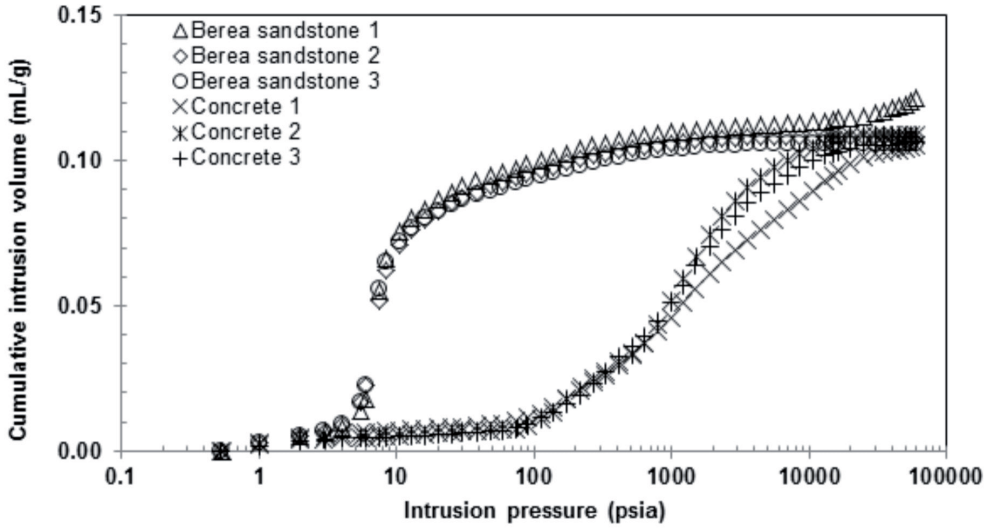

FIG. 1: Cumulative intrusion volume vs intrusion pressure for Berea sandstone

TABLE 2: Results of repeatability tests

Sample	MIP test	Porosity (%)		d_{50} (μm)		Average pore diameter d_a (μm)	
			avg±standard deviation		avg±standard deviation		avg±standard deviation
Berea sandstone	1	24.845	22.865±1.724	22.982	23.776±0.876	0.071	1.339±1.098
	2	22.051		23.631		1.954	
	3	21.698		24.716		1.992	
Concrete	1	20.811	21.077±0.239	0.140	0.161±0.018	0.036	0.059±0.023
	2	21.273		0.171		0.081	
	3	21.148		0.171		0.059	

described in this work. Note that the unconsolidated sediment samples were compacted in the gas diffusion chamber method (Peng et al., 2012), while they were loosely placed into the penetrometer for the MIP tests. The difference in packing and porosity could contribute to the difference in obtained diffusivity for these sediment samples.

4.3 Correlation of Gas Diffusivity with Porosity and Permeability

The exponential relationship between permeability and diffusivity, as shown in Fig. 3, is weak with a correlation coefficient value of R^2 = 0.549. However, it indeed indicates an increasing trend of diffusivity with the increase of permeability.

According to Eq. (2), we should obtain a linear relationship if we plot diffusivity versus porosity in log scale and the slope of the plot should give the value of m. Figure 4 shows the relationship between D' and porosity for our samples. The samples can be divided into two groups according to the different slope (m) value. One group, with m = 1.5, includes dolomite, limestone, Indiana sandstone, Berea sandstone and red brick and the remaining samples fall into another group with m = 2.5.

All four samples of unconsolidated sediment show relatively high m values (from 2.1 to 2.8), and the finer sediment tends to exhibit a larger m value, which is consistent with the conclusion of Peng et al. (2012). For consolidated samples, we plotted the diffusivity versus median pore diameter (d_{50}) and the two sample groups are shown with different legends in Fig. 5. We found that these two

TABLE 3: Porosity, average pore diameter, permeability, effective diffusion coefficient, diffusivity and m values of 14 samples

Sample	Porosity[a]	d_a[a] (μm)	Permeability (millidarcy)	D_e[b] (m^2/s)	D'[c]	m
Concrete (C1)	0.208	0.0357	1.45×10^{-2}	4.36×10^{-7}	0.021	2.45
Red brick	0.212	0.7345	1.42×10^{0}	1.83×10^{-6}	0.090	1.56
Limestone	0.145	0.3656	3.78×10^{1}	1.04×10^{-6}	0.051	1.54
Dolomite	0.091	0.1361	4.09×10^{-1}	4.35×10^{-7}	0.021	1.61
Indiana sandstone	0.167	0.2088	1.92×10^{2}	1.01×10^{-6}	0.049	1.68
Berea sandstone (B2)	0.221	1.9539	5.71×10^{2}	2.12×10^{-6}	0.104	1.50
Gray chalk	0.320	0.1149	1.22×10^{-1}	1.59×10^{-6}	0.078	2.24
White chalk	0.438	0.0915	2.23×10^{-1}	2.05×10^{-6}	0.100	2.78
Tuff	0.096	0.0252	7.33×10^{-4}	1.43×10^{-7}	0.007	2.12
Mudstone	0.196	0.0282	2.26×10^{-3}	3.37×10^{-7}	0.017	2.52
Hanford $<$ 2 mm	0.401	0.0937	3.69×10^{2}	1.86×10^{-6}	0.091	2.62
Hanford 500 μm–2 mm	0.137	0.0380	3.23×10^{-1}	2.89×10^{-7}	0.014	2.14
Hanford 75–500 μm	0.480	0.1590	7.06×10^{2}	3.10×10^{-6}	0.152	2.57
Hanford $<$75 μm	0.586	0.1947	2.83×10^{1}	4.46×10^{-6}	0.219	2.85

[a]Obtained from MIP

[b]Calculated at temperature 20°C for oxygen

[c]Calculated according to Eq. (2) with D_a = 2.04×10^{-5} m^2/s for oxygen

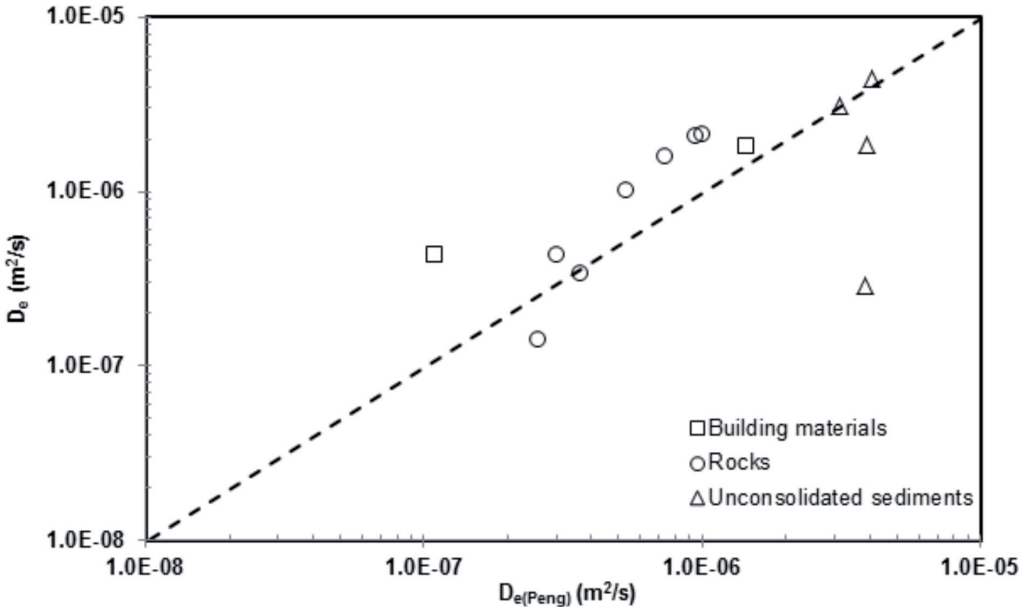

FIG. 2: Comparison between effective diffusion coefficients obtained in this work (D_e) and from reference ($D_{e(Peng)}$)

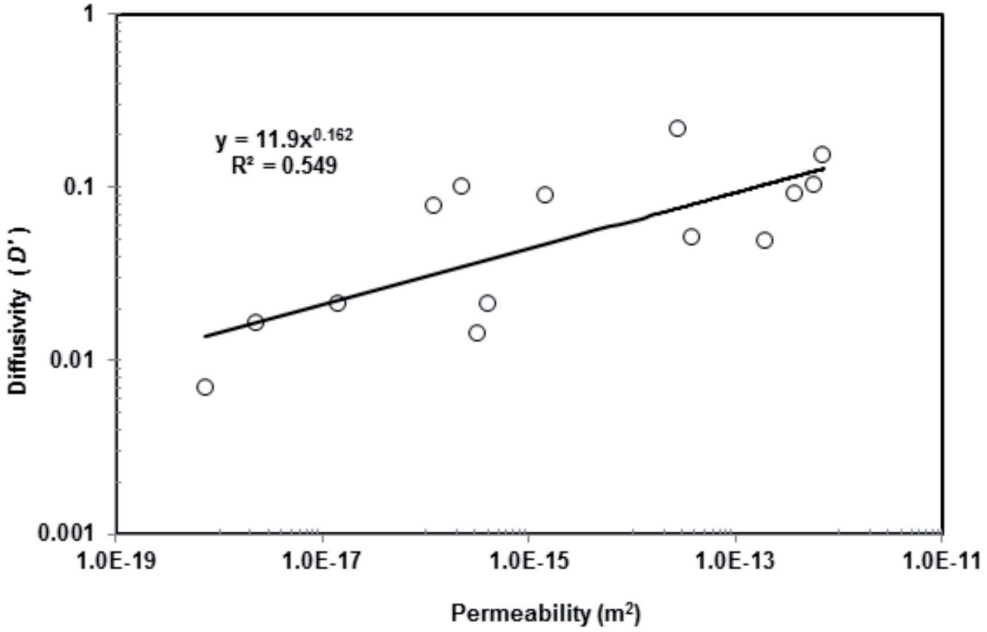

FIG. 3: Diffusivity (D') vs permeability

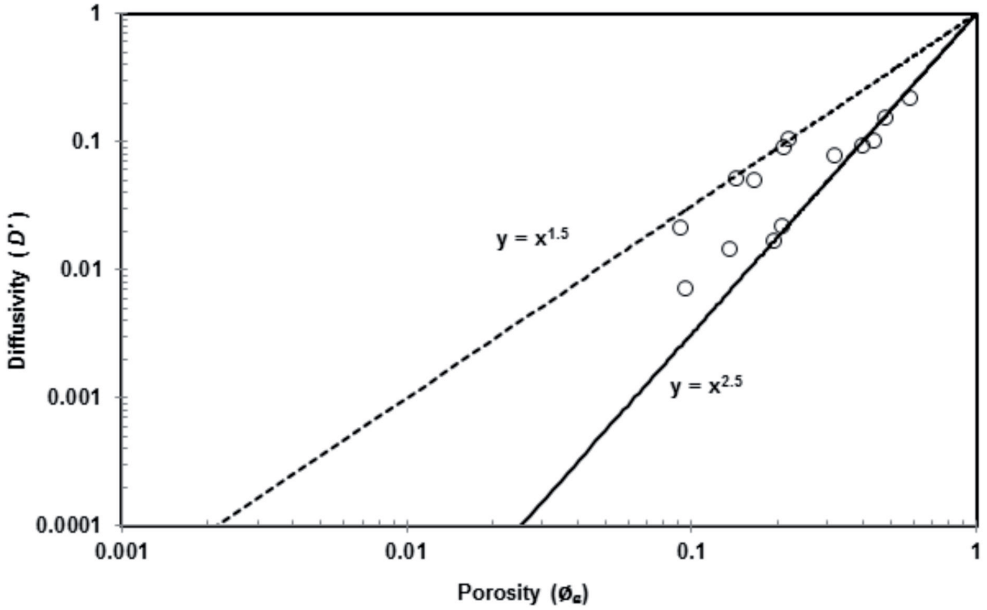

FIG. 4: Diffusivity (D') vs porosity ($\varnothing_a$) for our samples (two groups are divided according to the m value)

groups could also be separated by a cutoff d_{50} value of $\sim$0.5 μm. All the samples in the group with m = 1.5 have a relatively large d_{50} (>0.5 μm), while the samples of the m = 2.5 group have a smaller d_{50} (<0.5 μm); in other words, the tighter samples with d_{50} <0.5 μm tend to have the larger m value of 2.5. Compared with the scattered samples of the group with m = 1.5 (R^2 = 0.254), the tight samples exhibit a more organized behavior and display an

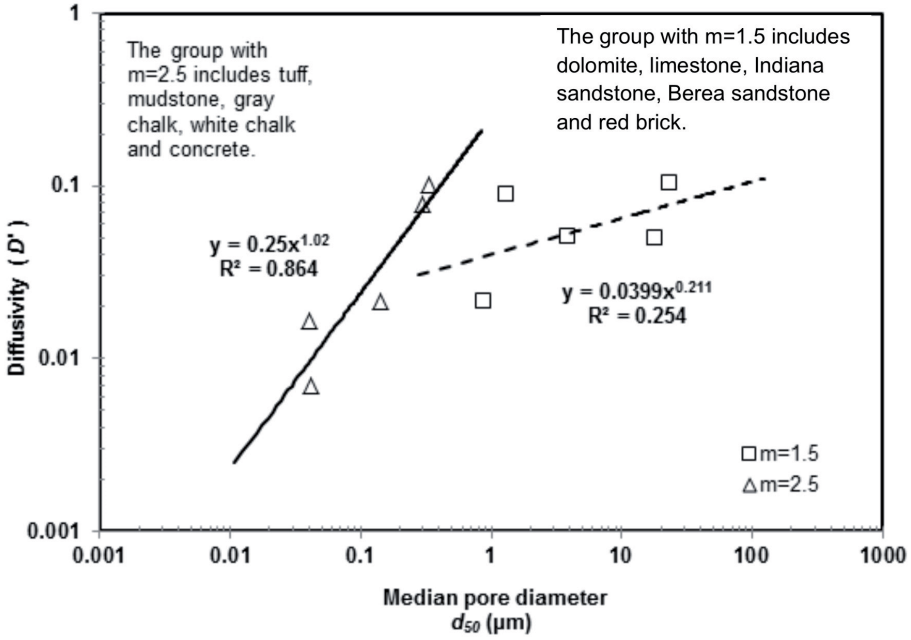

FIG. 5: Diffusivity (D') vs median pore diameter (d_{50}) for consolidated materials

exponential relationship between D' and d_{50} as shown in Fig. 5. This relationship can be summarized as

$$D' = 0.25 d_{50}^{1.017}, \tag{10}$$

where D' denotes diffusivity (dimensionless) and d_{50} is the median pore diameter in μm.

Although the MIP-derived gas diffusivities of building materials and unconsolidated sediments are comparable with the measured data (Fig. 2), the complexity of factitious building materials and the instability of unconsolidated sediments make it difficult to draw further conclusions, and interpretation of the complicated pore structures of these two types of porous medium is beyond the scope of this work. Accordingly the emphasis in the remainder of this section will be on the eight consolidated rock samples.

The relationship between permeability and porosity has been investigated and presented by many researchers (Chilingar et al., 1963; Ma and Morrow, 1996; Tiab and Donaldson, 2004). We plot the permeability versus porosity for eight rock samples together with two building materials in Fig. 6. The results show two different exponential relationships with relatively high R^2 (>0.9) for the two groups of samples with different m values. Again, dolomite, limestone, Indiana sandstone and Berea sandstone fall in the same group (m = 1.5), while tuff, mudstone, gray chalk and white chalk belong to the other group (m = 2.5).

For the sample group with m = 1.5, the following relationship exists:

$$k = 4 \times 10^{-7} \varphi_a^{8.53}, \tag{11}$$

where k is permeability in m^2 and φ_a is air-filled porosity.

For the group with m = 2.5, the relationship is

$$k = 6 \times 10^{-15} \varphi_a^{4.10}. \tag{12}$$

5. CONCLUSION

The objective of this work was to derive gas diffusivity from MIP data and to explore the correlation of diffusivity with permeability and porosity. The repeatability of MIP determinations was evaluated using Berea sandstone and concrete. In terms of average pore size, our results show that the consideration of Knudsen effect in many rocks is necessary. The effective diffusion coefficients (D_e) of three types of porous media (two building materials, eight consolidated rocks and four unconsolidated sediments) were calculated with established equations, using the information on average pore diameter (d_a) and porosity (φ_a), both of which are easily obtained by

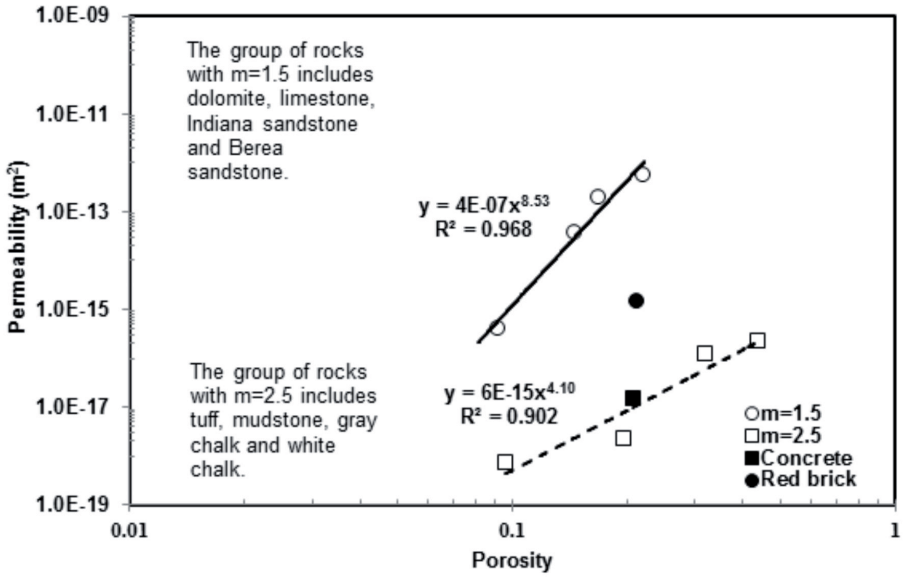

FIG. 6: Permeability vs porosity for consolidated materials

MIP. The results are basically in line with the experimental values obtained from gas diffusion tests. It should be pointed out that the method used to calculate D_e in this work is only applicable to samples with porosity between 0.05 and 0.95, as indicated in Eq. (8) of Carniglia (1986). However, except for extremely tight rocks such as granite, this method still has a wide applicability. Usually, one MIP test can be completed within 2 hours, which enhances the applicability of this method.

An increasing trend of diffusivity with increasing permeability was observable in our results, although the correlation was weak, as shown in Fig. 3. Diffusivity, calculated according to Eq. (2), was also used to obtain the m value, which is closely related to the pore structure. Two groups of samples were divided according to the m values (m = 1.5 vs m = 2.5). For the consolidated samples, these two groups could be further differentiated from each other according to the median pore diameter (d_{50}) obtained from MIP. When d_{50} is larger than $\sim$0.5 μm, the samples belong to the group with m = 1.5. Conversely, if d_{50} is less than $\sim$0.5 μm the sample probably has an m value of 2.5 and the diffusivity of this sample can be estimated according to Eq. (10). Moreover, the relationship between permeability and porosity was investigated for eight rock samples. Again, dolomite, limestone, Indiana sandstone and Berea sandstone in the group with m = 1.5 exhibited similar behavior, which can be expressed by Eq. (11), while tuff, mudstone, gray chalk and white chalk, all of which belonged to the group with m = 2.5, shared the same power-law form of Eq. (12).

ACKNOWLEDGMENTS

This research was supported by the Student Research Grant from Gulf Coast Association of Geological Societies, and RPSEA through the "Ultra-Deepwater and Unconventional Natural Gas and Other Petroleum Resources" program authorized by the U.S. Energy Policy Act of 2005. RPSEA (www.rpsea.org) is a nonprofit corporation whose mission is to provide a stewardship role in ensuring the focused research, development and deployment of safe and environmentally responsible technology that can effectively deliver hydrocarbons from domestic resources to the citizens of the United States. RPSEA, operating as a consortium of premier U.S. energy research universities, industry, and independent research organizations, manages the program under a contract with the U.S. Department of Energy's National Energy Technology Laboratory. The views and opinions of authors expressed herein do not necessarily state or reflect those of the United States Government or any agency thereof.

REFERENCES

Adler, P. M., Jacquin, C. G., and Thovert, J. F., The formation factor of reconstructed porous media, *Water Resour. Res.*, vol.

28, no. 6, pp. 1571–1576, 1992.

Archie, G. E., The electrical resistivity log as an aid in determining some reservoir characteristics, *Trans. AIME*, vol. **146**, pp. 54–62, 1942.

Boving, T. B. and Grathwohl, P., Tracer diffusion coefficients in sedimentary rocks: Correlation to porosity and hydraulic conductivity, *J. Contam. Hydrol.*, vol. **53**, pp. 85–100, 2001.

Busch, A., Alles, S., Gensterblum, Y., and Prinz, D., Carbon dioxide storage potential of shales, *Int. J. Greenhouse Gas Control*, vol. **2**, pp. 297–308, 2008.

Carniglia, S. C., Construction of the tortuosity factor from porosimetry, *J. Catal.*, vol. **102**, pp. 401–418, 1986.

Chilingar, G. V., Main, R., and Sinnokrot, A., Relationship between porosity, permeability, and surface areas of sediments, *J. Sediment. Petrol.*, vol. **33**, no. 3, pp. 759–765, 1963.

Cui, X., Bustin, A., and Bustin, R., Measurements of gas permeability and diffusivity of tight reservoir rocks: Different approaches and their applications, *Geofluids*, vol. **9**, pp. 208–223, 2009.

Cunningham, R. E. and Williams, R. J. J., Diffusion in gases and porous media, New York: Plenum, 1980.

Du, J. K., Bao, J., Hu, Q. H., and Ewing, R. P., Uranium release from different size fractions of sediments in Hanford 300 Area, Washington, USA, *J. Environ. Radioact.*, vol. **107**, pp. 92–94, 2012.

Ellison, A. H., Klemm, R. B., Schwartz, A. M., Grub, L. S., and Petrash, D. A., Contact angles of mercury on various surfaces and the effect of temperature. *J. Chem. Eng. Data*, vol. **12**, no. 4, pp. 607–609, 1967.

Evans, R. B., Watson, G. M., and Mason, E. A., Gaseous diffusion in porous media at uniform pressure, *J. Chem. Phys.*, vol. **35**, no. 6, pp. 2076–2083, 1961.

Gillham, R. W., Robin, M. L. J., Dytynyshyn, D. J., and Johnson, H. M., Diffusion of nonreactive and reactive solutes through fine-grained barrier materials, *Can. Geotech. J.*, vol. **21**, p. 541, 1984.

Grathwohl, P., *Diffusion in Natural Porous Media: Contaminant Transport, Sorption/Desorption and Dissolution Kinetics*, Boston: Kluwer Academic Publishing, p. 224, 1998.

Kast, W. and Hohenthanner, C. R., Mass transfer within the gas-phase of porous media, *Int. J. Heat Mass Transfer*, vol. **43**, pp. 807–823, 2000.

Katz, A. J. and Thompson, A. H., A quantitative prediction of permeability in porous rock, *Phys. Rev. B*, vol. **34**, pp. 8179–8181, 1986.

Katz, A. J. and Thompson, A. H., Prediction of rock electrical conductivity from mercury injection measurements, *J. Geophys. Res.*, vol. **92**, no. B1, pp. 599–607, 1987.

Kolodzie, S., Jr., Analysis of pore throat size and use of the Waxman-Smits equation to determine OOIP in Spindle Field, In *Proc. of Colorado Society of Petroleum Engineers, 55th Annual Fall Technical Conference*, Paper 9382, 1980.

Kumar, R. and Bhattacharjee, B., Assessment of permeation quality of concrete through mercury intrusion porosimetry, *Cem. Concr. Res.*, vol. **34**, pp. 321–328, 2004.

Ma, S. and Morrow, N. R., Relationships between porosity and permeability for porous rocks, Society of Core Analysts Conference Paper 9610, 1996.

Moore, C. A. and Alzayadi, A., *Theoretical considerations of movements of gases around sanitary landfills*, Report to U.S. EPA, 1975.

Moro, F. and Böhni, H., Ink-bottle effect in mercury intrusion porosimetry of cement-based materials, *J. Colloid Interface Sci.*, vol. **246**, pp. 135–149, 2002.

Mu, D., Liu, Z., and Huang, C., Determination of the effective diffusion coefficient in porous media including Knudsen effects, *Microfluid. Nanofluid.*, vol. **4**, pp. 257–260, 2008.

Peng, S., Hu, Q., and Hamamoto, S., Diffusivity of rocks: Gas diffusion measurements and correlation to porosity and pore size distribution, *Water Resour. Res.*, vol. **48**, W02507, doi:10.1029/2011WR011098, 2012.

Pollard, W. G. and Present, R. D., On gaseous self-diffusion in long capillary tubes, *Phys. Rev.*, vol. **73**, pp. 752–774, 1948.

Rojas, E., Pérez-Rea, M., Gallegos, G., and Leal, J., A porous model for the interpretation of mercury porosimetry tests, *J. Porous Media*, vol. **15**, no. 6, pp. 517–530, 2012.

Rolston, D. E. and Moldrup, P., Gas diffusivity, In *Methods of Soil Analysis. Part 4—Physical Methods*, Dane, J. H., and Topp, G. C., Eds., Madison, Wisconsin: Soil Science Society of America, Inc., pp. 1113–1139, 2002.

Seo, J., Kato, S., Ataka, Y., and Zhu, Q., Evaluation of effective diffusion coefficient in various building materials and absorbents by mercury intrusion porosimetry, in *Proc. of The 10th International Conference on Indoor Air Quality and Climate*, 2005.

Shackelford, C. D., Laboratory diffusion testing for waste disposal—A review, *J. Contam. Hydrol.*, vol. **7**, pp. 177–217, 1991.

Shi, D. and Winslow, D. N., Contact angle and damage during mercury intrusion into cement paste, *Cem. Concr. Res.*, vol. **15**, pp. 645–654, 1985.

Swanson, B. F., A simple correlation between permeabilities and mercury capillary pressures, *J. Pet. Technol.*, vol. **33**, pp. 2498–2504, 1981.

Tiab, D. and Donaldson, E. C., *Petrophysics—Theory and Practice of Measuring Reservoir Rock and Fluid Transport Properties*, Amsterdam: Elsevier, 2004.

Tsakiroglou, C. D. and Payatakes, A. C., Characterization of the pore structure of reservoir rocks with the aid of serial sectioning analysis, mercury porosimetry and network simulation,

Adv. Water Resour., vol. **23**, pp. 773–789, 2000.

Washburn, E. W., Note on a method of determining the distribution of pore sizes in a porous material, *Proc. Natl. Acad. Sci. U. S. A.*, vol. **7**, pp. 115–116, 1921.

Webb, P. A., *An Introduction to the Physical Characterization of Materials by Mercury Intrusion Porosimetry with Emphasis on Reduction and Presentation of Experimental Data*, Micromeritics Instrument Corporation, 2001.

Westermarck, S., Juppo, A. M., Kervinen, L., and Yliruusi, J., Pore structure and surface area of mannitol powder, granules and tablets determined with mercury porosimetry and nitrogen adsorption, *Eur. J. Pharm. Biopharm.*, vol. **46**, pp. 61–68, 1998.

Zhou, J. A., Ye, G. A., and van Breugel, K., Characterization of pore structure in cement-based materials using pressurization-depressurization cycling mercury intrusion porosimetry (PDC-MIP), *Cem. Concr. Res.*, vol. **40**, no. 7, pp. 1120–1128, 2010.